

See discussions, stats, and author profiles for this publication at: <https://www.researchgate.net/publication/260572193>

Transition of the Coastal and Estuarine Storm Tide Model to an Operational Storm Surge Forecast Model: A Case Study of the Florida Coast

Article in *Weather and Forecasting* · August 2013

DOI: 10.1175/WAF-D-12-00076.1

CITATIONS

7

READS

91

5 authors, including:



Keqi Zhang

Florida International University

63 PUBLICATIONS **2,823** CITATIONS

[SEE PROFILE](#)



Yuepeng Li

Florida International University

17 PUBLICATIONS **218** CITATIONS

[SEE PROFILE](#)



Huiqing Liu

North Carolina State University

18 PUBLICATIONS **342** CITATIONS

[SEE PROFILE](#)



Jamie Rhome

NOAA/National Hurricane Center

24 PUBLICATIONS **583** CITATIONS

[SEE PROFILE](#)

Some of the authors of this publication are also working on these related projects:



Create new project "Applications of LIDAR data" [View project](#)



Lynnhaven River Restoration Project [View project](#)

Transition of the Coastal and Estuarine Storm Tide Model to an Operational Storm Surge Forecast Model: A Case Study of the Florida Coast

KEQI ZHANG

Department of Earth and Environment, and International Hurricane Research Center, Florida International University, Miami, Florida

YUEPENG LI AND HUIQING LIU

International Hurricane Research Center, Florida International University, Miami, Florida

JAMIE RHOME AND CRISTINA FORBES

NOAA/National Weather Service/National Centers for Environmental Prediction/National Hurricane Center, Miami, Florida

(Manuscript received 30 July 2012, in final form 27 February 2013)

ABSTRACT

The operational forecast demands and constraints of the National Hurricane Center require that a storm surge model in research mode be tested against a benchmark model such as Sea, Lake, and Overland Surges from Hurricanes (SLOSH) for accuracy, computation time, and numerical stability before the model is used for operational forecasts. Additionally, the simulated results must be in a geographic information system format to facilitate the usage of computed storm surge for various applications. This paper presents results from a demonstration project to explore the pathway for the transition of the Coastal and Estuarine Storm Tide (CEST) model to an operational forecast model by testing CEST over SLOSH basins in Florida. The performance and stability of CEST were examined by conducting simulations for Hurricane Andrew (1992) and more than 100 000 synthetic hurricanes for nine SLOSH basins covering the Florida coast and Lake Okeechobee. The results show that CEST produces peak surge heights similar to those from SLOSH. Additionally, CEST has proven to be numerically stable against all synthetic hurricanes and the computation time of CEST is comparable to that of SLOSH. Therefore, CEST has the potential to be used for operational forecasts of storm surge. The potential of producing more detailed real-time surge inundation forecasts was also investigated through the simulations of Andrew's surge on various grids with different cell sizes. The results indicate that CEST can produce 48-h forecasts using a single processor in about 40 min over a grid generated by reducing the cell edge size of the SLOSH grid by 4 times.

1. Introduction

One of the major hazards caused by hurricanes in the United States is storm surge flooding, which can damage buildings and infrastructure, block escape routes, and drown people in low-lying coastal areas along the Atlantic and Gulf coasts. In 2005, storm surge from Hurricane Katrina impacted the Louisiana, Mississippi, Alabama, and Florida coasts, resulting in the death of about 1200 people and \$108 billion in property damage (Blake et al. 2011). To avoid loss of life because of storm

surge flooding, evacuation plans have been developed and enacted in U.S. coastal areas (Forbes and Rhome 2011). Evacuation zones are determined by a combination of coastal topographic elevations and predicted storm surge heights over the land, which are computed by the National Weather Service's (NWS) numerical storm surge model: Sea, Lake, and Overland Surges from Hurricanes (SLOSH). The National Hurricane Center (NHC) performs real-time storm surge forecasts using SLOSH during the hurricane season to provide critical information for evacuation decision making in response to storms that threaten the U.S. coastline (Glahn et al. 2009).

There are two ways to perform real-time surge forecasts: 1) pregenerated composite and 2) real-time simulation methods. In the pregenerated composite

Corresponding author address: Keqi Zhang, Dept. of Earth and Environment, Florida International University, 11200 SW 8th St., Miami, FL 33199.
E-mail: zhangk@fiu.edu

method, storm surge inundations for a coastal area (basin) are precomputed based on a set of climatologically generated synthetic hurricanes that can affect the basin. Storm surge forecasts are generated by selecting the precomputed storm surge from a hurricane closest to the forecasted hurricane through a lookup table listing the parameters of synthetic hurricanes or by combining precomputed surge heights from synthetic hurricanes using a statistical method (Irish et al. 2011). The advantage of this method is that surge simulations can be performed in advance and are less limited by computation time. Therefore, more computationally intensive models, such as the Advanced Circulation (ADCIRC; Luettich et al. 1992) model and Finite Volume Coastal Ocean Model (FVCOM; Chen et al. 2003), which cover large coastal areas with high-resolution grids, can be employed in this manner. The disadvantage of the pregenerated composite method is that actual storms may not match precomputed ones because the synthetic hurricanes cannot perfectly represent real storms. Often, a reasonable estimate of peak storm surge heights along the coast can be derived by this method (Irish et al. 2011). However, a reliable estimate of the surge flooding extent that is critical for evacuation is difficult to achieve because of variability in the wind and track parameters.

The second method generates the storm surge forecast by running hydrodynamic models in a real-time fashion based on the actual hurricane forecasts rather than synthetic ones. The advantage of the real-time simulation method is that it takes into account the variability of wind parameters and the track as the hurricane approaches land. The disadvantage is that the resolution and coverage of the model domain are limited by the available computational resources because multiple model executions in a short period are required to accommodate the uncertainty in the hurricane forecast. The strict constraint on computation time allows only a handful of hydrodynamic models with high computational efficiency to perform real-time surge forecasts.

SLOSH is one example of the hydrodynamic models that can be used to perform real-time forecasts because of its low computational complexity due to the utilization of a linearized momentum equation. The SLOSH model has served the nation well for several decades, but recent studies suggest that improvement in surge forecasts could be made through updating the model physics and algorithms (Bunya et al. 2010; Forbes et al. 2007; Rego and Li 2008). For example, the SLOSH model suffers from several drawbacks, such as excluding advective acceleration and horizontal diffusion terms in the momentum equation (Jelesnianski et al. 1992; Murty

1984), neglecting the effect of land cover on inundation, and insufficient spatial resolutions to fully resolve the details of overland flooding. The further refinement of the model grid is limited by the allowable reduction in the time step that is required to maintain the numerical stability of the explicit scheme used by SLOSH in terms of the Courant–Friedrichs–Lewy condition. The utilization of a filtering method can improve the stability of the explicit scheme (Taylor and Forbes 2011), but cannot completely remove the limitation set by the explicit scheme.

Many numerical models for coastal and oceanic hydrodynamics have been developed for simulating tide, wind-driven circulation, and storm surge over the past two decades. Examples of these models include the Princeton Ocean Model (POM; Blumberg and Mellor 1987); the Curvilinear Hydrodynamics in Three Dimensions (CH3D) model (Sheng 1987); the ADCIRC model (Luettich et al. 1992), the Environmental Fluid Dynamics Code (EFDC) model (Hamrick 1992); the Unstructured Tidal, Residual, and Intertidal Mudflat (UnTRIM) model (Casulli and Walters 2000); FVCOM (Chen et al. 2003); the Eulerian–Lagrangian Circulation (ELCIRC) model (Zhang et al. 2004); the Coastal and Estuarine Storm Tide (CEST) model (Zhang et al. 2008); and the Semi-Implicit Eulerian–Lagrangian Finite Element (SELFE) model (Zhang and Baptista 2008). These models solve the full momentum equations together with the continuity equation by maintaining nonlinear advective acceleration and diffusion terms. These models and their extensions also include the wetting–drying component and have recently been applied to the simulation of overland flooding (Bunya et al. 2010; Forbes et al. 2009; Forbes et al. 2010; Huang et al. 2010; Shen et al. 2006; Sheng et al. 2010; Xie et al. 2004; Xu et al. 2010). However, these models cannot be used directly for operational surge forecasts because most of them are developed in research mode and have not been tested to meet the requirements of an operational center such as the NHC. The lack of a clear research-to-operation (R2O) pathway for hydrodynamic models hinders the usage of cutting-edge hydrodynamic models for operational surge forecasting.

Although the Joint Hurricane Testbed program at the NHC provides a funding opportunity for a R2O transition of hurricane-related products, few studies place emphasis on the R2O transition process of a hydrodynamic model for surge forecasting because 1) the requirements for real-time surge forecasting have not been clearly defined and 2) the procedure to perform the R2O transition has not been explored. The main objective of this research is to explore a possible pathway for transitioning a storm surge model in a research mode

into an operational one using CEST as an example. The secondary objective is to identify the requirements of operational storm surge forecasts at the NHC to facilitate the interaction between research and operational communities. This paper is arranged as follows. Section 2 describes the requirements of a hydrodynamic model for performing real-time surge forecasts. Section 3 briefly presents the SLOSH and CEST models. Section 4 describes the procedure to convert a SLOSH basin to the CEST grid. Section 5 compares the SLOSH and CEST simulations on the Miami basin and other basins in Florida, and presents and discusses the CEST simulations on the refined grids. Section 6 consists of discussion. Section 7 draws conclusions.

2. Requirements of operational storm surge forecasting

There is considerable uncertainty in forecasting hurricanes (e.g., their tracks, intensities, and sizes) that drive storm surge models. Exact flood magnitude and extent cannot be determined in advance because of this uncertainty, even if hydrodynamic models are very accurate in predicting storm surges. In addition, evacuation orders have to be issued well before hurricanes make landfall because time is needed to evacuate residents. The NWS overcomes these difficulties by using conservative approaches by first generating the maximum envelope of water (MEOW) in a coastal area. The MEOW is composed of the maximum surge at each grid cell computed by SLOSH based on a large ensemble of storms of a given category, track direction, and forward speed with varying sizes and landfall locations (Shaffer et al. 1989). Then, the maximum of MEOWs (MOMs) for a given category of hurricanes, indicating coastal areas that could potentially be flooded by this category of storms from all possible directions, is generated. Finally, the evacuation zones are created through hurricane evacuation studies based on the storm surge threat depicted by the MEOWs and MOMs. In reality, the extent of flooding from a single event is usually less than those from the MEOWs and MOMs corresponding to the category of the event. This is because the MEOWs–MOMs are intended to help develop evacuation plans rather than forecast a single event.

Because of the inherent uncertainty associated with pinpointing the exact nature and landfall location of a given hurricane, it is necessary to develop conservative evacuation zones. However, if more forecast accuracy could be attained, more efficient hurricane evacuations could be executed with less societal disruption and costs. One improvement in hurricane evacuation decision making is the use of Probabilistic Hurricane Storm

Surge (P-Surge) forecasts (Taylor and Glahn 2008), which are produced based on a possible range of hurricane intensities, sizes, and tracks determined by the NHC's forecast and its uncertainty, rather than based on MOMs for synthetic hurricanes from all directions. The P-Surge model generates more realistic forecasts of the possible ranges of inundation magnitudes and extents for a hurricane than the forecasts based on MOMs. Real-time storm surge simulations are required to produce P-Surge products because the NHC updates the hurricane forecast/advisory every 6 h. Obviously, the forecasts of storm surges are only useful if they are available to users before the arrival of the next advisory. The ideal situation for emergency managers is that the surge forecasts are available immediately after the NHC issues a hurricane advisory so they can use the advisory and surge forecasts for decision making. Although it is impractical to derive surge forecasts immediately after issuing an advisory, the needs of emergency managers for fast responses require that the storm surge guidance based on an updated advisory be available in minutes rather than hours.

The NWS offers three-tiered products for decision making (Fig. 1) related to storm surge flooding. For planning and mitigation work prior to 120 h of landfall, the usage of MOMs is recommended. Both MEOWs and MOMs, which provide potential storm surge for a given hurricane category at a regional level, are recommended between 48 and 120 h before landfall. The usage of P-Surge and MEOWs is recommended for possible and potential storm surge scenarios during a period from 0 to 48 h before landfall, which is often critical for decision making. To produce reliable real-time probabilistic forecasts of surge flooding, thousands of simulations using storms of varying tracks, intensities, sizes, and forward speeds for affected basins need to be completed (Glahn et al. 2009). The simulations and the creation of P-Surge are completed in approximately 20–30 min using National Oceanic and Atmospheric Administration's (NOAA) operational forecasting supercomputer. Additionally, because the NHC generates and iteratively refines the hurricane forecast between advisories, unplanned quick diagnostic predictions need to be completed within 5–10 min in response to adjustments to the hurricane forecast. Currently, the NHC performs "as needed" diagnostic forecasts by running SLOSH using multicore PC workstations. Often, several surge forecasts need to be generated to accommodate the uncertainty in the forecast of hurricane track, intensity, size, and forward speed. This approach is called a mini-MEOW (or miniensemble) forecasting method. The ability to generate real-time P-Surge and mini-MEOW forecasts places a strict requirement on the computation time of hydrodynamic models.

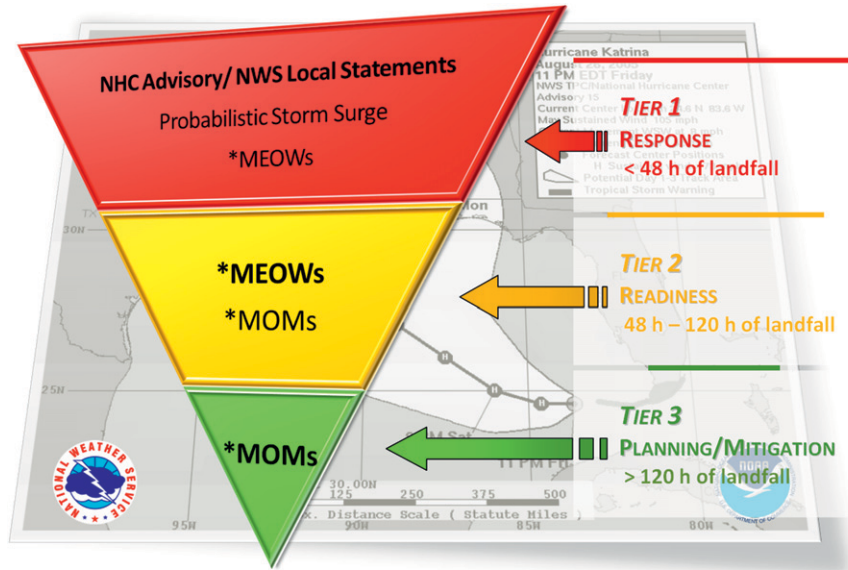


FIG. 1. The storm surge products from the NHC and the recommended timelines to use these products.

In addition to time constraints on the storm surge forecast, the modeling approach must be consistently employed over the U.S. Atlantic and Gulf coasts. The simulations have to be robust without becoming unstable during the forecast, which means that the model must undergo rigorous testing using a set of climatologically generated hurricanes that could affect the U.S. Atlantic and Gulf coasts. Finally, the results of surge simulations should be available in geographic information system (GIS) format to facilitate the usage of surge flooding data across many platforms by evacuation planners, decision makers, and the scientific community.

3. SLOSH and CEST models

a. Hydrodynamic model

Two-dimensional (2D) models are often used to model storm surges to reduce the time complexity of numerical computation. With the Boussinesq and hydrostatic pressure approximations, the 2D depth-integrated momentum equations for shallow water in a Cartesian coordinate system can be expressed by

$$\begin{aligned} & \frac{\partial HU}{\partial t} + \frac{\partial HU^2}{\partial x} + \frac{\partial HUV}{\partial y} \\ & = fHV - g \frac{\partial}{\partial x} \left(\zeta + \frac{\Delta P_a}{\rho g} \right) - \frac{\tau_b^x}{\rho} + \frac{\tau_s^x}{\rho} + A_h \frac{\partial^2 HU}{\partial x^2} \\ & + A_h \frac{\partial^2 HU}{\partial y^2} \quad \text{and} \end{aligned} \quad (1)$$

$$\begin{aligned} & \frac{\partial HV}{\partial t} + \frac{\partial HUV}{\partial x} + \frac{\partial HV^2}{\partial y} \\ & = -fHU - g \frac{\partial}{\partial y} \left(\zeta + \frac{\Delta P_a}{\rho g} \right) - \frac{\tau_b^y}{\rho} + \frac{\tau_s^y}{\rho} + A_h \frac{\partial^2 HV}{\partial x^2} \\ & + A_h \frac{\partial^2 HV}{\partial y^2}. \end{aligned} \quad (2)$$

The continuity equation is

$$\frac{\partial \zeta}{\partial t} + \frac{\partial HU}{\partial x} + \frac{\partial HV}{\partial y} = 0, \quad (3)$$

where x and y are the horizontal coordinates, t represents time, H is the water depth from the still water level to the bottom, ζ is the water surface elevation reference to the still water level, U and V are depth-integrated velocities along the x and y directions, f is the Coriolis parameter, g is the gravitational acceleration, ΔP_a is the atmospheric pressure drop, ρ is the water density, A_h is the horizontal eddy diffusivity, τ_b^x and τ_b^y are bottom stresses, and τ_s^x and τ_s^y are surface wind stresses.

b. SLOSH model

SLOSH is a 2D finite-difference model developed by the NWS in the early 1980s (Jelesnianski et al. 1992), but it is not simply a depth-averaged model. The bottom stress is not determined by the depth-averaged velocity. Instead, it is based on a vertical velocity profile that considers the effects of Ekman drift (Jelesnianski 1970;

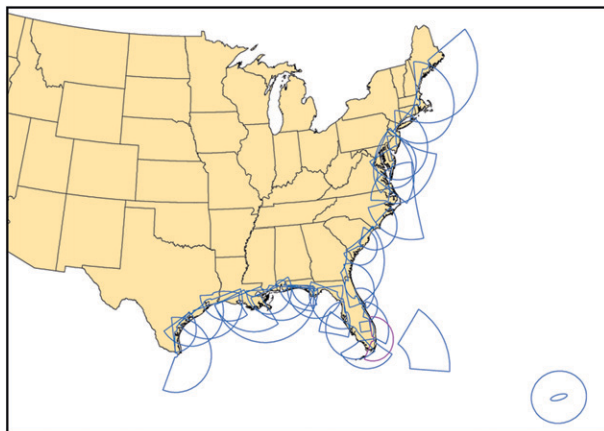


FIG. 2. SLOSH basins along the U.S. Atlantic and Gulf coasts. The purple outline is the Miami basin.

Kim and Chen 1999). SLOSH incorporates water level gradients, but excludes advective acceleration and horizontal diffusion terms in momentum Eqs. (1) and (2). The model is forced by surface wind stress and atmospheric pressure drop and does not dynamically simulate tides, although efforts are under way at the NWS's Meteorological Development Laboratory (MDL) to incorporate tides into SLOSH (Haase et al. 2011). SLOSH employs specialized momentum and continuity equations and a set of rules based on the relationship between water flows and water level elevations of neighboring cells to handle wetting–drying processes (Jelesnianski et al. 1992). In the initial flooding of a grid cell, the flow is driven only by gravity forces, and the surface driving forces are ignored. During ebb surge, if the computed water level elevation at a cell is equal to or below the topographic elevation, the cell is set to be dry. Since it is difficult to construct and manage one SLOSH grid of sufficient resolution for conducting evacuation studies for the entire U.S. Atlantic and Gulf coasts, the coastal area from Maine to Texas is divided into 37 overlapping basins for surge simulation (Fig. 2) (Conver et al. 2010; Glahn et al. 2009). To cover a large area and maintain the fine resolution near the coast without losing computational efficiency, a polar, elliptical, or hyperbolic grid with gradually varying cell size is chosen to represent a basin (i.e., model domain). A model grid generated this way usually covers a region extending from the inland area possibly flooded by storm surge to the deep water about 150–200 km offshore. The cell sizes of the model grid typically range from hundreds of meters in coastal areas to several kilometers in the open ocean. The inputs of the SLOSH model are a mix of ASCII and binary files and the outputs are all in binary formats. Extensive efforts in the past 30 yr have been

made to build and maintain the 37 SLOSH basins along the U.S. Atlantic and Gulf coasts. SLOSH has been tested by numerous runs for historical and synthetic hurricanes with various intensities, sizes, moving speeds, and forward direction (Jelesnianski et al. 1992), setting up a solid foundation for performing real-time surge forecasting and serving as a benchmark model for surge model comparisons.

Both natural and man-made linear features such as topographic ridges, barrier islands, levees, rivers, and canals play important roles in reducing or enhancing overland surge flooding. The widths of these linear features are often less than the size of a grid cell. The SLOSH model introduces subgrid features including barrier, cut, and one-dimensional (1D) flow to account for the effects of linear features (Jelesnianski et al. 1992). A barrier is a thin “wall” along a cell boundary with user-specified elevation that blocks storm surge flows, a 1D flow represents a channel with a user-specified width proportional to the edge width of a grid cell, and a cut is the location along a channel where the width of the flow with banks changes (Conver et al. 2010).

c. CEST model

The CEST model is a finite-difference model developed by Zhang et al. (2008) through modifying the explicit algorithms of the POM model (Blumberg and Mellor 1987) to simulate estuarine and coastal flooding induced by hurricanes. The CEST model solves the continuity and full momentum equations, which are forced by winds, atmospheric pressure drops, and astronomical tides or a time series of water levels at open boundaries. The depth-averaged 2D CEST model over orthogonal curvilinear grids was used to simulate storm surges in this study. The radiation open boundary condition was employed to allow waves to propagate out of the model domain (Blumberg and Kantha 1983). To improve the computational efficiency and stability of the model, a semi-implicit scheme is employed to produce a discrete form of the control equations (Casulli and Chen 1992). Only the water pressure gradient and bottom friction items are solved implicitly and the remaining terms are treated explicitly. With varying cell sizes, the curvilinear grid is more flexible in generating fine grid cells at the coast and coarse ones at the open ocean than a SLOSH grid because the orthogonal grid lines can be in any shape and do not have to follow polar, elliptical, or hyperbolic shapes. The CEST model uses a mass-balanced algorithm based on accumulated water volume to simulate the wetting–drying process. The model can also run on conformal grids such as those used by SLOSH without modification of the numerical algorithms. The inputs and outputs of the CEST model are in

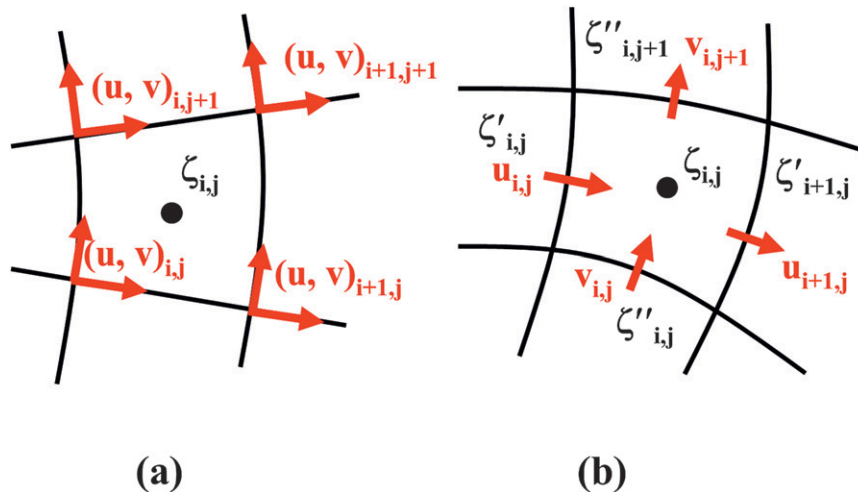


FIG. 3. (a) The semistaggered Arakawa B grid used by the SLOSH model and (b) the modified fully staggered Arakawa C grid for the CEST model.

Network Common Data Form (NetCDF; <http://www.unidata.ucar.edu/software/netcdf/>). A set of tools in Matlab (www.mathworks.com) have been developed to convert input files created in ArcGIS (www.esri.com) into NetCDF files and to convert output NetCDF files into ArcGIS shapefiles for displaying and analyzing simulated surges.

The CEST model was verified by comparing calculated surges from historical storms such as Hurricanes Andrew, Camille, Hugo, and Wilma with field observations (Zhang et al. 2008; Zhang et al. 2012). The SLOSH's parametric wind (SWind) model was employed by CEST to generate wind fields for modeling storm surges from Andrew, Camille, and Hugo, while a time series of wind fields (H*Wind, the real-time hurricane wind analysis system), generated by NOAA's Hurricane Research Division, based on field measurements (Powell et al. 2009; Powell et al. 1998) was used to model the storm surge from Wilma. The measured maximum high-water-mark elevations from hurricanes Andrew, Camille, Hugo, and Wilma are about 5, 7, 6, and 5 m, respectively, above the North American Vertical Datum of 1988 (NAVD88). The root-mean-square differences between computed and observed high-water levels for these four hurricanes are 0.44, 0.58, 0.47, and 0.39 m, respectively. The CEST model has also been employed to perform preliminary real-time forecasts of storm surges based on advisory tracks for Hurricanes Isabel in 2003 and Katrina in 2005. The comparison of computed surges with tidal gauge records and high-water-mark measurements indicates that the model largely reproduced the inundation pattern generated by Hurricanes Isabel and Katrina.

4. Conversion of SLOSH basins to CEST grids

Since maintenance of a surge modeling system, especially basin development and maintenance, is expensive and the products such as MEOWs and MOMs for SLOSH basins have been extensively used in emergency management communities at the federal, state, and county levels, it would be difficult for the NHC and its partner agencies to immediately switch from SLOSH products to those from another hydrodynamic model. One way for a new operational model to alleviate this transition problem is to develop the capability of performing surge simulations over existing SLOSH basins and to demonstrate the ability to reproduce associated MEOW and MOM products. This would allow an operational center such as the NHC to potentially adopt an additional modeling system without incurring the huge costs associated with transitioning, building, and maintaining a new set of model grids. Therefore, the first step in exploring the R2O transition process for converting a research hydrodynamic modeling system such as CEST into an operational model is to test the feasibility of running the model over existing SLOSH basins.

The computation scheme of the SLOSH model is based on the Arakawa B grid (Jelesnianski et al. 1992; Purser and Leslie 1988; Taylor and Forbes 2011) with velocity components at the four corners of a grid cell and the elevation at the center (Fig. 3a). The following set of shapefiles (Fig. 4) has been created in ArcGIS by the MDL to maintain and update SLOSH basins (Conver et al. 2010):

- 1) a grid-cell polygon shapefile;
- 2) a cell center point shapefile with the average cell elevation for the cell center;

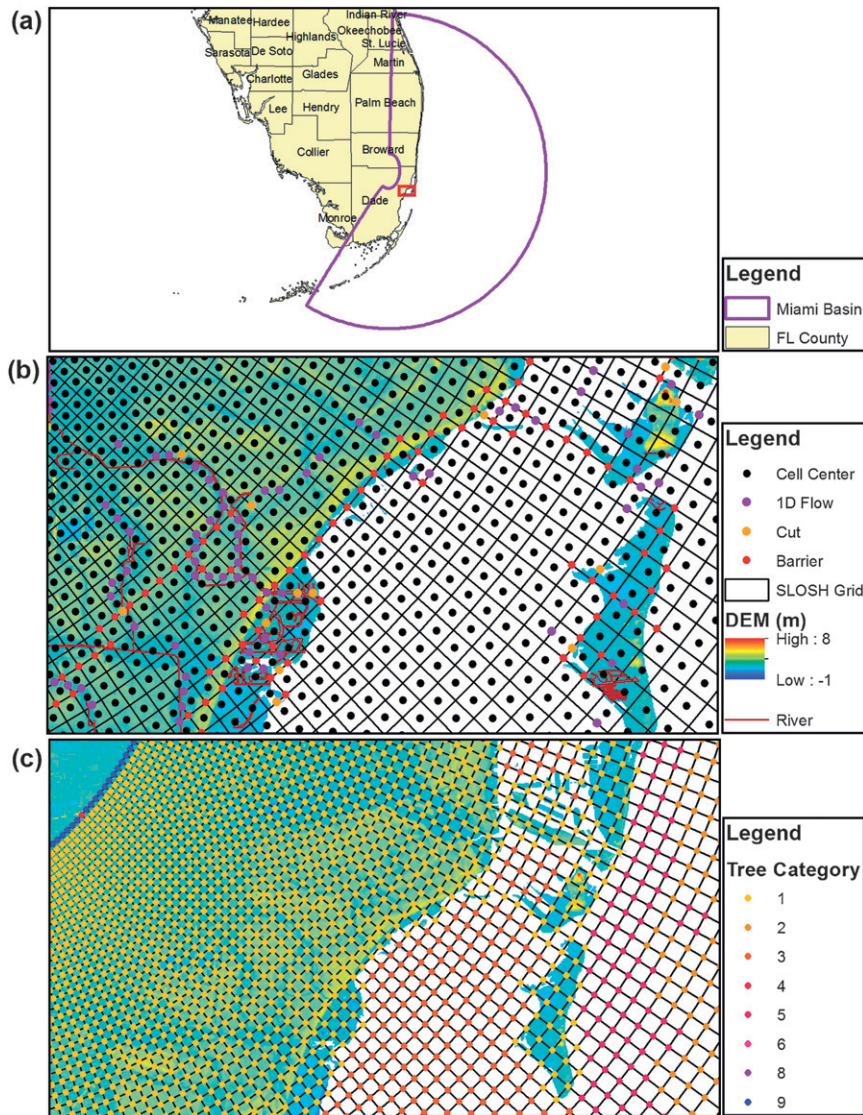


FIG. 4. (a) The shape of the Miami basin used in the SLOSH model. Displayed are (b) grid cell, cell center, barrier, cut, and 1D flow, and (c) tree category for the basin. The DEM and rivers and canals are also displayed in (b) to help visualize the barriers and flows.

- 3) a 1D flow point shapefile with property indicating two types of 1D flows, where 1D flow with a width value of -1 represents the water flow that crosses the entire cell when the cell is wet and 1D flow with width value of $0.1-0.9$ indicates that the flow moves through a channel limited by banks with width of $0.1-0.9$ times of the cell edge length; the position of the 1D flow point coincides with the centers of cell edges;
- 4) a cut point shapefile, which is used to connect 1D flows with channels of varying widths; cut points are on the centers of cell edges;
- 5) a barrier point shapefile representing levees and barrier islands with points coinciding with the vertices of grid cells;
- 6) a momentum point shapefile, which represents the maximum elevation height of the four surrounding grid cells, and is used by the SLOSH model to determine the water flowing between cells; the momentum points coincide with the vertices of grid cells; and
- 7) a tree value point shapefile for computing surface wind stress at the momentum points. Tree values are divided into three main categories:
 - (i) land and channels:
 - value 1 for lake and tree—forest land with elevation between 0 and 11.0m (36ft) in reference to NAVD88;

- value 3 for lake only—nonforested land with elevation between 0 and 11.0 m, as well as channels and bays below 0 m; and value 4 for high terrain—land with elevation ≥ 11.0 m;
- (ii) oceans:
value 2 for deep water—the water with elevation < -9.1 m (-30 ft); and
value 5 for shallow water—the water with elevation ≥ -9.1 m;
- (iii) boundary values (along the edges of the model grid):
value 4 for solid wall (no flow)—all land;
value 6 for static height—elevation ≤ -9.1 m;
value 8 for intermediate—elevation between -9.1 and -22.9 m (-75 ft); and
value 9 for shallow—elevation from 0 to -9.1 m.

The computation scheme of the CEST model is based on the modified Arakawa C grid (Blumberg and Mellor 1987; Purser and Leslie 1988) with velocity components at the four edges of a grid cell and the elevation at the center (Fig. 3b). The elevations at the four edges are also included in the numerical scheme to simulate wetting and drying processes using the accumulative volume method (Zhang et al. 2008). The attributes of a CEST grid cell include horizontal coordinates of four vertices and the center, the five elevation values at the center and four edges, four velocities of water flows perpendicular to the edges, a tree category, and five flags for four edges and the cell indicating whether they are dry or wet. To run CEST on a SLOSH grid, a SLOSH grid was converted into the CEST grid using the following procedure:

- 1) grid coordinate—extract the grid coordinates from the SLOSH shapefile and create the grid for CEST;
- 2) cell center depth—set the center depth of a CEST cell to be the depth of SLOSH cell center;
- 3) edge depth—set edge depths of a CEST cell by averaging center depths of two adjacent CEST cells;
- 4) barrier depth—update the depth of an edge by averaging the depths of two adjacent SLOSH barrier points that are connected by the edge;
- 5) flow depth:
 - (i) update the center depths of the cells at the left H_L and right H_R sides of the edge coinciding with a flow point using a width-weighting method,

$$\begin{aligned} H_L &= wH_{\text{flow}} + (1 - w)H_{\text{LO}} \quad \text{and} \\ H_R &= wH_{\text{flow}} + (1 - w)H_{\text{RO}}, \end{aligned} \quad (4)$$

where w is the ratio of the flow width to the edge width, H_{flow} is the depth of the SLOSH flow point, H_{LO} is the original center depth of the cell at the left side of the edge, and H_{RO} is the original center depth of the cell at the right side of the edge;

- (ii) update the depth H_E of the edge that coincides with the flow point using center depths of two adjacent cells,

$$H_E = \max(H_L, H_R); \quad (5)$$

- 6) cut depth—update edge and center depths using the same method for flow depth;
- 7) tree flag—set up the tree flag of a CEST cell based on the value of SLOSH tree point at the top-right vertex of the CEST cell, where the tree flag is only used for computation of the wind field in CEST; similar to SLOSH, the wind speed in a cell covered by vegetation is adjusted using a coefficient C_T based on the ratio of the surge water depth D to the vegetation height H_T (Jelesnianski et al. 1992),

$$C_T = \begin{cases} \frac{D}{H_T}, & D < H_T; \\ 1, & D \geq H_T \end{cases}; \quad (6)$$

the effect of trees on the wind speed decreases based on this equation as the water submerges the vegetation gradually;

- 8) Manning coefficients—calculate Manning coefficients for ocean and land grid cells; the CEST model uses the Chezy formula (LeMehaute 1976; Zhang et al. 2012) with Manning's roughness coefficient to calculate bottom stresses; the Manning coefficients for ocean grid cells are computed by an empirical formula based on the water depth H ,

$$n_w = \begin{cases} 0.02, & 0 < H < 1 \text{ m} \\ 0.01/H + 0.01, & H \geq 1 \text{ m} \end{cases}, \quad (7)$$

or set up to be constants, for example,

$$n_w = C, \quad (8)$$

where C ranges from 0.01 to 0.03. Manning coefficients for grid cells over the land were estimated according to the 2006 National Land Cover Database (NLCD) created by the U.S. Geological Survey (USGS) (Fry et al. 2011). Table 1, which is modified from Mattocks and Forbes (2008), lists the Manning coefficient for each category of land cover. Since the spatial resolution of the NLCD is 30 m, which is much smaller than the cell size of a SLOSH grid, an

TABLE 1. Manning coefficients for various categories of land cover (modified from Mattocks and Forbes, 2008).

NLCD class No.	NLCD class name	Manning coef
11	Open water	0.020
12	Perennial ice/snow	0.010
21	Developed open space	0.020
22	Developed low intensity	0.050
23	Developed medium intensity	0.100
24	Developed high intensity	0.130
31	Barren land (rock/sand/clay)	0.090
32	Unconsolidated shore	0.040
41	Deciduous forest	0.100
42	Evergreen forest	0.110
43	Mixed forest	0.100
51	Dwarf scrub	0.040
52	Shrub/scrub	0.050
71	Grassland/herbaceous	0.034
72	Sedge/herbaceous	0.030
73	Lichens	0.027
74	Moss	0.025
81	Pasture/hay	0.033
82	Cultivated crops	0.037
90	Woody wetlands	0.140
91	Palustrine forested wetland	0.100
92	Palustrine scrub/shrub wetland	0.048
93	Estuarine forested wetland	0.100
94	Estuarine scrub/shrub wetland	0.048
95	Emergent herbaceous wetlands	0.045
96	Palustrine emergent wetland (persistent)	0.045
97	Estuarine emergent wetland	0.045
98	Palustrine aquatic bed	0.015
99	Estuarine aquatic bed	0.015

average Manning coefficient n_a for a grid cell was calculated using

$$n_a = \frac{\sum_{i=1}^N (n_i \alpha) + n_w \beta}{N\alpha + \beta}, \quad (9)$$

where n_i is the Manning coefficient value of an NLCD pixel within a model grid cell, α is the area of an NLCD pixel, N is the total number of NLCD pixels within a model cell, and n_w is the Manning coefficient for the oceanic area β that is not covered by NLCD pixels.

5. Comparison of SLOSH and CEST simulations

a. Simulations on the original SLOSH grid

The second step in exploring the R2O transition process for converting CEST into an operational model is to compare the CEST and SLOSH simulations for

individual storm events. The Miami basin and Hurricane Andrew (1992) were selected to examine simulations on a SLOSH grid for a single event because a high-resolution Miami basin was developed in 2009 and the elevations of the basin have been updated using high quality light detection and ranging (lidar) data collected in 2007. It would be better to use the version of the Miami basin that was established in the 1990s in order to represent the topographic and land cover conditions during Andrew. Unfortunately, the vertical error in the old USGS digital elevation model (DEM) that was used in that version of the basin has a much larger influence on the computation of the inundation than the difference in topography caused by the geomorphic processes and the development from 1992 to 2007. In addition, while it is desirable to compare SLOSH and CEST for multiple individual storm events, only Andrew was available in the study area with the level of detailed observations required for comparison; thus, the SLOSH and CEST simulations for Andrew are selected to compare the model performance. More than 200 measurements of high-water marks on the buildings and trees and the debris lines indicating inland inundation extents were collected by the USGS (Murray 1994). These high-water-mark measurements and debris lines were converted into shapefiles in ArcGIS to facilitate the validation of surge models (Zhang et al. 2008).

Both a parametric hurricane wind model and a time series of observed wind fields, H*Wind (Powell et al. 2009; Powell et al. 1998), can be used to compute wind stresses in the CEST model. H*Wind only provides snapshots of the wind field every 2–6 h, but the instantaneous wind field is needed for storm surge computation by the model at each time step. Thus, the wind fields between two adjacent H*Wind fields are generated using a bilinear interpolation in space and a linear interpolation in time based on the center positions of two H*Wind fields and the values of H*Wind fields. Two simulations of Andrew's surges were conducted on the SLOSH grid using the CEST model in order to examine the effects of hydrodynamic algorithms and wind field on storm surges. The first simulation used the parametric SLOSH wind as would be done in forecast mode, while the second simulation used the interpolated H*Wind to examine the effect of the difference in wind fields on storm surge computation. Each simulation, starting at 1100 coordinated universal time (UTC) 21 August and ending at 1500 UTC 25 August 1992, continued for 100 h. For a comparison purpose, a third simulation was also performed by using SLOSH with its parametric wind. The simulation based on H*Wind was not conducted with the SLOSH model because of the

limitation on the input of the wind field in SLOSH. The mean sea level prior to Hurricane Andrew in August 1992 at Haulover Pier is about -0.25 -m reference to the NAVD88. The elevations of SLOSH grid cells in the current Miami basin are referenced to NAVD88; thus, the still water level was set up to be -0.25 m. The tidal component was not included in the simulations in order to be consistent with SLOSH. Manning coefficients for the underwater portion of the basin were empirically set to be 0.015 for a range of 0.01–0.03 based on the comparison of CEST simulations with field observations.

Comparison of simulated peak surge heights from the SLOSH model with observed elevations of high-water marks shows that SLOSH underestimates surges from Andrew by 12% overall, even though SLOSH overpredicts surges in the 1–3-m range (Fig. 5). The computed inundation boundary at the southern coast of Biscayne Bay is located much farther inland than the measured debris line (Fig. 6). To analyze the variability of the errors in computed peak surge heights, the mean square error (MSE) of computed peak surges versus measured surges was decomposed into the mean square due to bias (MSB) and mean square due to deviations (MSD) (Table 2). The highly scattered peak surge heights from the simulation (Fig. 5a), as indicated by a large MSD value, lead to a root-mean-square (RMS) error of 0.64 m.

The CEST simulation using the SLOSH parametric wind model produced less scattered computed peak surges (Fig. 5b) with an MSD value of 0.15 m^2 , whereas the simulation considerably underestimated peak surge heights by 22% with an MSB value of 0.20 m^2 . The combination of MSB and MSD generates an RMS error of 0.59 m. The overall pattern of simulated peak surge heights from the CEST model is similar to that from the SLOSH model (Fig. 6). However, the area of peak surge heights greater than 2 m from the CEST simulation is smaller than that from the SLOSH simulation. Comparison of the spatial pattern of computed peak surges with the debris line indicates that the CEST simulation produced the inundation extent closer to the observed one. The CEST simulation using H*Wind generated higher storm surge values, reduced the MSB of computed peak surges (Fig. 5c) to 0.05 m^2 , and increased MSD to 0.20 m^2 , producing an RMS error of 0.50 m. The bias of computed peak surge heights was reduced, but the computed peak surge still underestimated the measured ones by 12%, which is probably caused by the wave effect that was not included in the simulation. The improvement of the CEST simulation using H*Wind indicates that an accurate wind field is crucial for modeling storm surges. Since H*Wind, which is generated by the analysis of observations is not available for a forecast

product, one of the efforts to advance the surge forecast in the future should focus on improving parametric wind models.

The third step in exploring the R2O transition process for converting CEST into an operational model is to compare the CEST and SLOSH simulations for multiple storms and recreate existing products (i.e., MOM and MEOW). Nine SLOSH basins including Jacksonville (EJAX), Cape Canaveral (CO2), Palm Beach (PB3), Miami (HMI3), Florida Key (EKE2), Fort Myers (EFM2), Tampa Bay (ETP3), Apalachicola Bay (AP2), and Lake Okeechobee (EOK2), which cover most of the coast of Florida and the Lake Okeechobee area, were used in this study (Fig. 2). To produce MEOW and MOM data for a given basin, the NHC generates from about 10 000 to 15 000 synthetic tracks of hurricanes with various approaching directions, forward speeds, radii of maximum winds, and pressure drops. The CEST model was tested on the nine Florida basins using the NHC tracks 1) to evaluate computational efficiency, 2) to examine the numerical stability of the model, and 3) to generate MEOWs and MOMs to compare with those from SLOSH. The CEST model completed 72-h simulations on SLOSH basins within 2 min with time steps of 15–60 s in most cases by using a single 2.5-GHz Intel Xeon processor. This computation time of CEST is comparable to that of SLOSH, even though CEST's algorithms are more complicated. This is because a larger time step can be employed in CEST because of its use of a semi-implicit algorithm.

The stability of the CEST model was examined by analyzing model results for a basin using the following procedure. First, a surge height deviation shapefile for each MEOW was created by subtracting the neighborhood average surge height from the surge height at a grid cell. The neighborhood average surge height of a grid cell was computed by averaging the surge heights of eight neighbors of the cell. The surge height deviation shapefile for each individual storm was also created using the same method. Second, the surge height deviation map for each MEOW was displayed and examined in ArcGIS. If an abnormal deviation was found, we traced the error source by analyzing the surge deviation maps for the individual storms. If no abnormal deviation in a MEOW was found, the representative surge height deviation maps for the individual storms in the MEOW were examined for further verification. The analysis of model results indicated that the CEST model ran successfully on the nine SLOSH basins for more than 100 000 tracks without occurrence of numerical instabilities. The major reason for such a good performance by CEST on numerical stability tests is that the water depth values of model grid cells are already

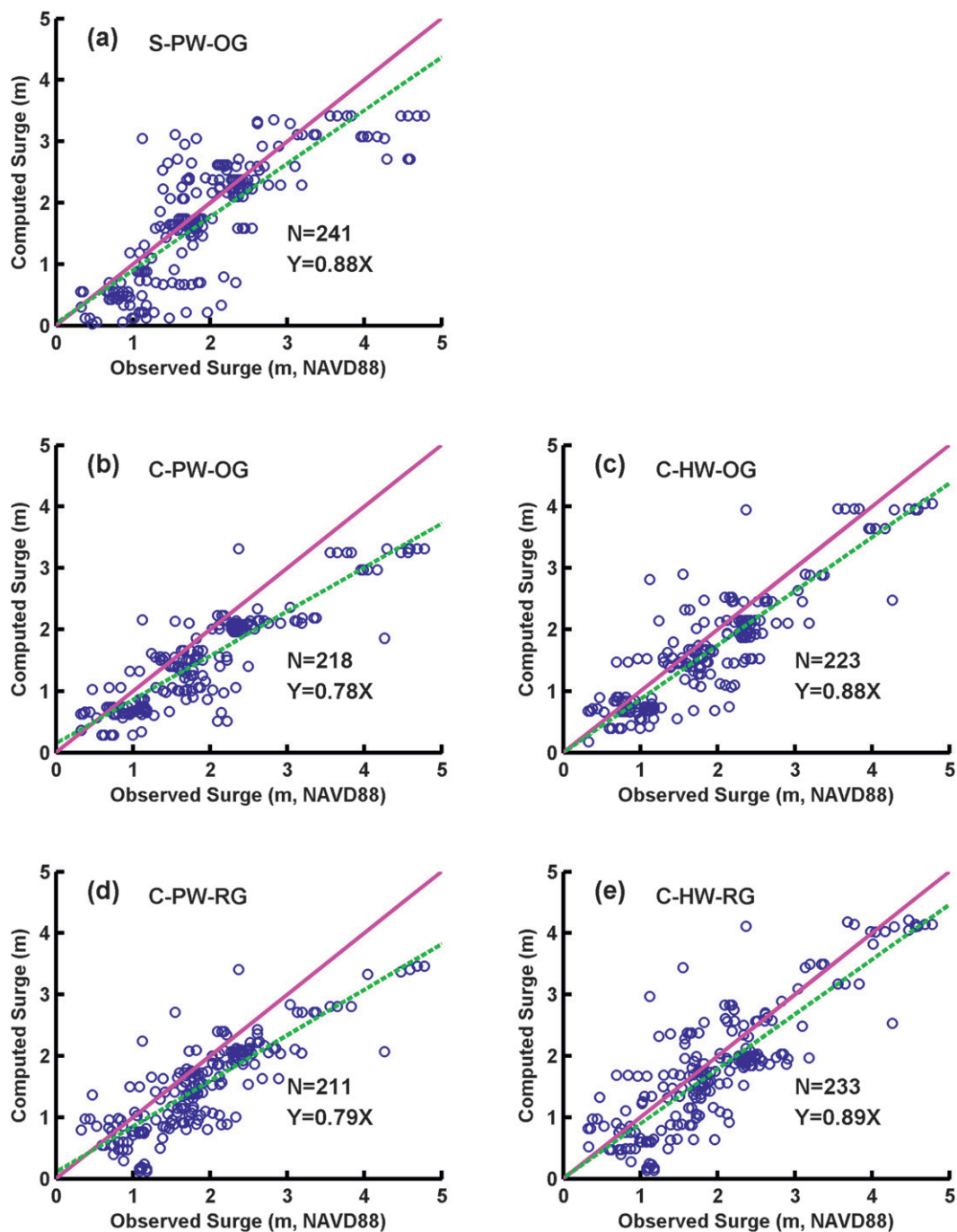


FIG. 5. Observed vs computed peak surge heights using (a) SLOSH with the parametric wind and the original grid (S-PW-OG), (b) CEST with the parametric wind and the original grid (C-PW-OG), (c) CEST with H*Wind and the original grid (C-HW-OG), (d) CEST with the parametric wind and the refined grid (C-PW-RG), and (e) CEST with H*Wind and the refined grid (C-HW-RG). The solid purple line represents perfect simulations and the dashed green line represents the linear regression line that is forced to pass through the origin. The refined grid was derived by reducing the cell edge size of the original SLOSH grid by a factor of 4. The observed peak surge heights were the elevations of high-water marks left on the buildings and trees by storm tides. The total number of observed and computed surge pairs is slightly different for each simulation because the computed surge does not reach the locations with observed surges in several cases, especially when the observations are located in the area adjacent to canals and creeks far inland.

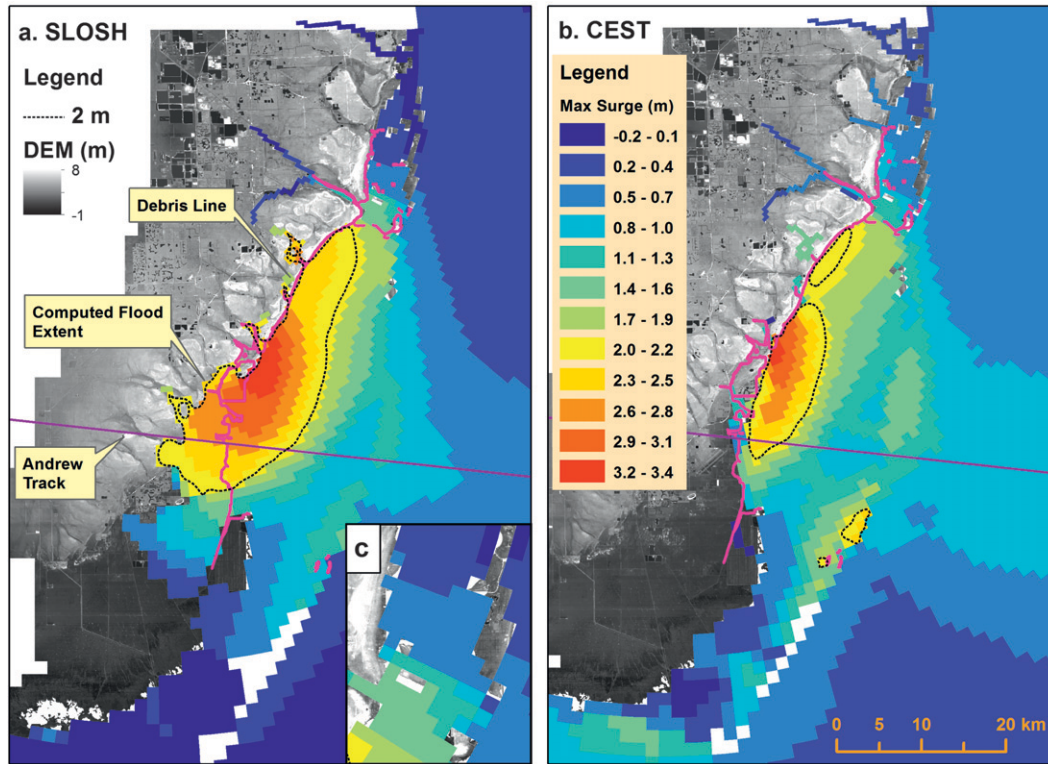


FIG. 6. Spatial distribution of simulated peak surge heights for Hurricane Andrew from (a) SLOSH and (b) CEST using the parametric wind. Inset (c) shows the zoomed-in view of peak surge heights surrounding the barrier island, including Miami Beach.

smoothed and tested by the MDL and the NHC during the basin building process. In addition to the ratio of grid-cell size versus time step, the major factors that may cause the instability of the CEST model include abrupt variations of bathymetry, topography, and the Manning coefficients. Previous numerical experiments show that CEST is sensitive to the abrupt changes of water depths at the open boundaries. A GIS analysis indicates that water depths at the open boundaries of the nine Florida SLOSH basins are all gradual.

In most cases, the CEST model produced MEOWs and MOMs comparable to those generated by SLOSH. For example, the MOM maps of the Apalachicola Bay

basin for category 5 hurricanes indicate that CEST and SLOSH produce similar inundation extents, while the peak surge heights from SLOSH are slightly higher than those from CEST along the coast on the right side of the basin (Fig. 7). There are several cases in which MEOWs and MOMs from CEST and SLOSH have notable differences. For example, the CEST model produces slightly higher peak surges, but with much smaller inundation extents based on the MOM maps of the Miami basin for category 5 hurricanes (Fig. 8). The extent of the CEST MOM is close to the range of Miami-Dade County’s current evacuation zone C, which is for category 4 and 5 hurricanes, while the

TABLE 2. Statistics of computed vs observed peak surge heights.

Model	Wind	Grid	RMSE (m)	MSE* (m ²)	MSB (m ²)	MSD (m ²)
SLOSH	SWind	Original	0.64	0.41	0.05	0.36
CEST	SWind	Original	0.59	0.35	0.20	0.15
CEST	H*Wind	Original	0.50	0.25	0.05	0.20
CEST	SWind	Refined	0.59	0.35	0.14	0.21
CEST	H*Wind	Refined	0.57	0.32	0.04	0.28

* $MSE = (1/n) \sum_{i=1}^n (y_i - x_i)^2 = (\bar{y}_i - \bar{x}_i)^2 + (1/n) \sum_{i=1}^n (y_i - \bar{y}_i)^2 + (1/n) \sum_{i=1}^n (x_i - \bar{x}_i)^2 - (2/n) \sum_{i=1}^n (x_i - \bar{x}_i)(y_i - \bar{y}_i) = MSB + MSD$, where n is the total number of observations, x is the observed elevations of high-water marks, y is the computed peak surges at the locations of high-water marks. In addition, MSB is represented by the first term in the above equation and MSD is represented by the remaining three terms.

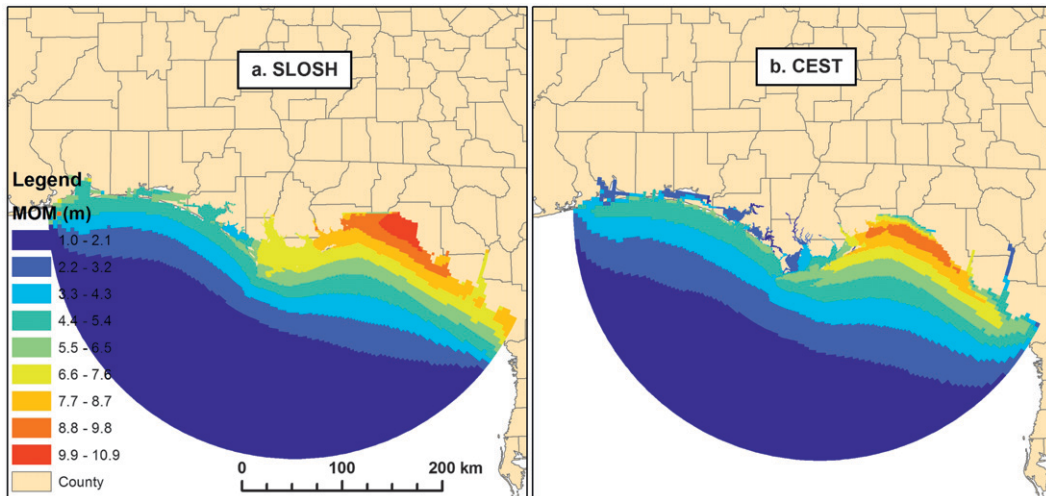


FIG. 7. The MOM maps for category 5 hurricanes generated from (a) SLOSH and (b) CEST simulations for the Apalachicola Bay basin show a similar spatial pattern.

SLOSH MOM covers more inland areas. The Miami-Dade evacuation zones were not based entirely on SLOSH MOMs, but empirically developed by F. Reddish, the former emergency management coordinator for Miami-Dade County (J. Lord, Miami-Dade County Department of Emergency Management, 2012, personal communication).

b. CEST simulations on the refined SLOSH grid

The fourth step in exploring the R2O transition process for converting CEST into an operational model is to examine the potential of improving surge forecasts by conducting CEST simulations on refined SLOSH grids. That is, does the candidate model have the ability to meet the future needs of an operational center by allowing higher-resolution grids while retaining computational stability, accuracy, and efficiency? To explore whether CEST's semiexplicit numerical algorithm can meet these needs, the simulation of Andrew's surges was performed on various grids derived by reducing the cell size of the SLOSH grid. Figure 9 shows a grid that was generated by reducing the edge size of an original SLOSH grid cell by 4 times. The elevations of the ocean cells in the model basin were calculated by interpolating the elevations of the original SLOSH grid cells, while the elevations of the land cells in the model basin were updated using the lidar data collected by the Florida Division of Emergency Management in 2007. The shapes of barrier islands at Miami Beach and navigation channels next to Dodge Island are clearly resolved in the refined grid, making it unnecessary to utilize subgrid features such as barriers and flows to represent many linear features with widths less than the cell sizes of the original SLOSH grid.

The refined grid also allows better representation of the complex river and canal systems in south Florida (Fig. 10). This was achieved by first creating a shapefile in ArcGIS for the edges of flow cells by intersecting canal polygons with the cell edges of the model grid. Then, the width of a river or canal on a flow cell edge was calculated and assigned into the associated attribute table of the shapefile for flow cell edges. Finally, automatically generated cell edges for rivers and canals were edited in ArcGIS to remove redundant edges or add new edges to maintain the connection of flow cells. The effects of flood control gates can also be included into the simulation by assigning the gate elevations to the edges of flow cells.

Two simulations of Hurricane Andrew using both the SLOSH parametric wind model and wind forces from H*Wind analyses were carried out with CEST for 100 h on the refined grid without flood control gates. Compared to the simulation generated using the SLOSH wind, the simulation generated using H*Wind produces a larger area of storm surge and higher storm surge values (Figs. 5d, 5e, and 11), which is the same as the simulations on the original grid. Although the bias between the computed and observed peak surge heights on the refined grid is reduced slightly (Table 2), the RMS errors of two simulations on the refined grid do not improve because of increased MSD values. Overall, the inundation patterns and extents on the original and refined grids derived by using the same method to compute wind fields (i.e., SLOSH wind or H*Wind) are similar (Figs. 6 and 11). However, there are large differences in the computed inundation extents from the original and refined grids in some areas. For example,

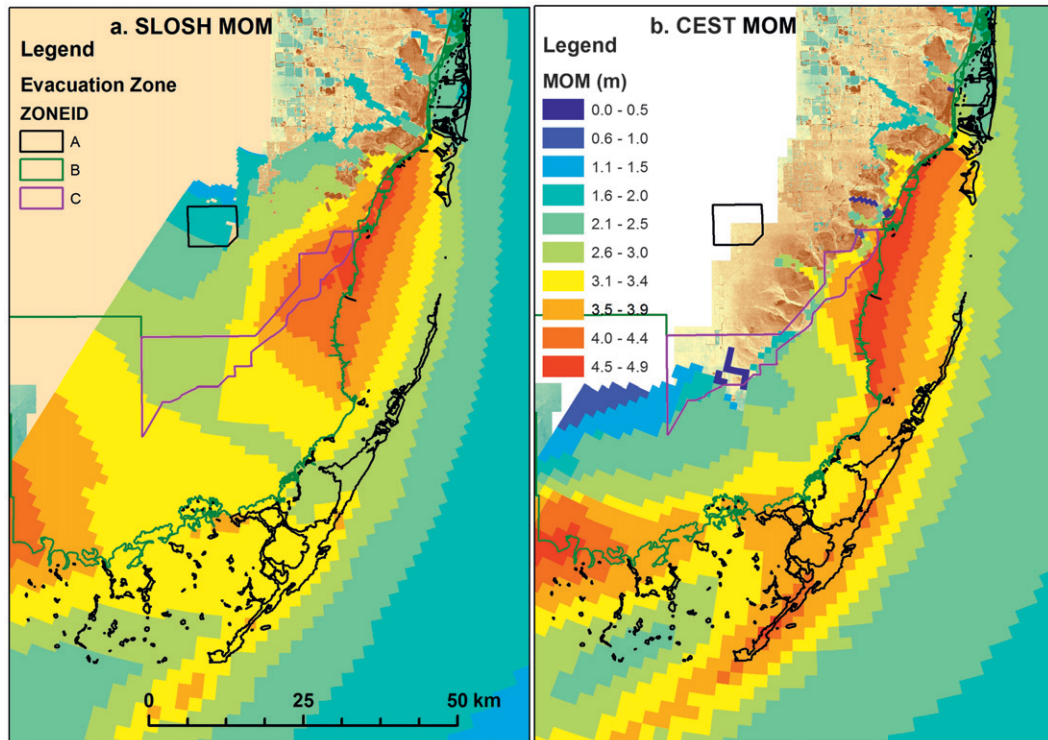


FIG. 8. The MOM maps for category 5 hurricanes generated from (a) SLOSH and (b) CEST simulations for the Miami basin exhibit different spatial patterns.

Fig. 11c shows that most areas on the bay side of Miami Beach on the refined grid are not flooded during Hurricane Andrew because of blockage of storm surge by the barrier island on the east side and Dodge Island on the south side (Fig. 9). In contrast, large areas of Miami Beach are flooded based on the simulation on the original grid because the barrier island and Dodge Island are not fully resolved in the original coarse grid (Fig. 6c).

The utilization of the grid with a reduced cell size improves the computation of the inundation extent, but incurs more computation time. To examine the effect of grid resolution on computation time, we conducted a series of numerical simulations on the grids with various cell sizes for a period of 48 h (Table 3). The simulations on the grid derived by reducing the cell edge size of the original SLOSH grid by 4 times were completed in about 43–54 min by using 30- and 20-s time steps; thus, CEST on this grid can still be used for the deterministic real-time forecast. Table 3 also shows that the CEST model is capable of running the simulation on a grid of more than 3 000 000 cells with a single processor. Therefore, it will be possible to run simulations on even finer-resolution grids when the speed of a single computer processor becomes faster in the future or if the CEST algorithms are parallelized to fit a machine with multiple processors.

6. Discussion

The differences between SLOSH and CEST algorithms in handling of wetting and drying processes, overland bottom friction, and nonlinear terms have varying effects on the computation of storm surges in the open ocean, shallow water, and land areas. The differences in the peak surge heights computed by SLOSH and CEST are usually small for the open ocean and large in the shallow bays and lagoons. This spatial difference in peak surge heights is probably caused by including, versus ignoring, the nonlinear terms in the momentum equations or by the differences in wetting and drying algorithms, and needs to be further investigated for each SLOSH basin to determine their contributions. The overland inundation extents and magnitudes from CEST are less than those from SLOSH in some cases. This difference in inundation is mainly caused by the disparity in the handling of the bottom friction. The overland flow of CEST is influenced by the Manning coefficients, which are determined based on land cover types. In the CEST model, the surge inundation is reduced in the heavily vegetated and highly developed areas because of increased bottom friction, rendering a more realistic simulation (Zhang et al. 2012). In

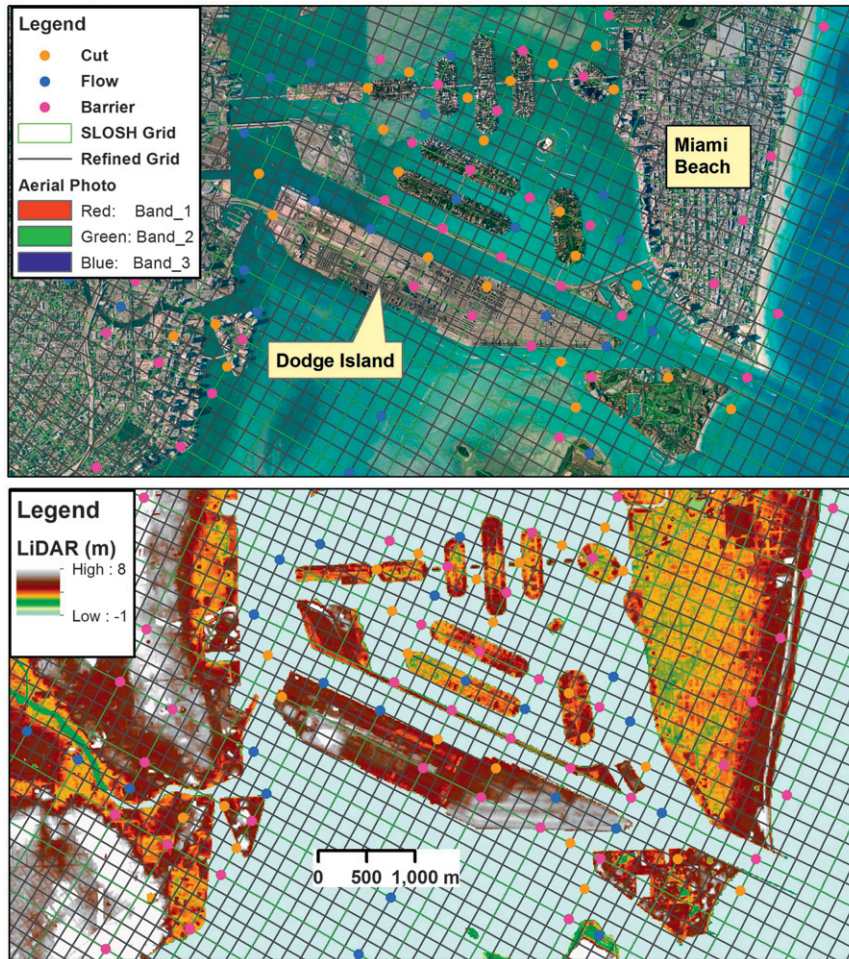


FIG. 9. The original SLOSH grid and the refined grid derived by reducing the edge size of an original grid cell by a factor of 4 overlaid on (top) the aerial photograph and (bottom) the lidar topography at the Miami Harbor area. The cell size of the original SLOSH grid is about 500–700 m in the coastal Miami area, while the cell size of the refined grid is about 150–170 m.

contrast, the bottom friction of the SLOSH model does not include the effects of variations in land cover. Additionally, the CEST model uses a minimum accumulation water volume in a grid cell to determine whether the cell is wetting during the flood surge, which generates a slower inundation process than the SLOSH model.

The Manning coefficient is an important parameter used by the CEST model that is not available in a SLOSH basin. Over the land, the computation of Manning coefficients based on the national land cover dataset is somewhat subjective. More field measurements of overland flooding processes on different types of land cover are needed to verify the current Manning coefficients. It is also problematic to determine the Manning coefficients for the shallow coastal water. Theoretically, the Manning coefficients for the underwater portion

should be based on categories of bottom floors. Unfortunately, there is no national dataset that classifies underwater bottom floors. The CEST model uses either a constant Manning coefficients ranging from 0.01 to 0.03 or Manning coefficients for the ocean bottom that vary with water depths [Eq. (7)]. A constant Manning coefficient of 0.015 for the ocean bottom and the varying Manning coefficients based on Eq. (7) produce similar results for the case of Hurricane Andrew. Ideally, several historical hurricanes with abundant field observations for each basin are needed to calibrate Manning coefficients and verify the model; unfortunately, very few basins have such field measurements. Numerous field observations have been collected by various agencies including the USGS, NOAA, the U.S. Army Corps of Engineers, and the Federal Emergency Management Agency for recent hurricanes after realizing the importance of field

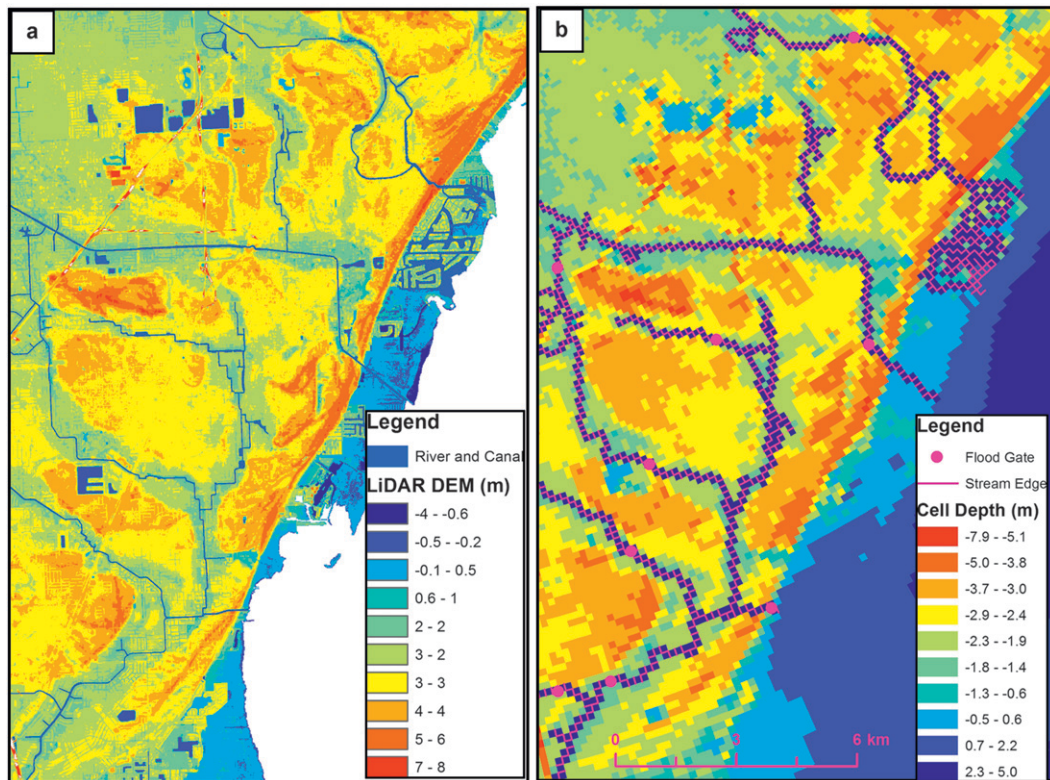


FIG. 10. (a) The lidar DEM and river and canals for the Miami basin and (b) the elevations of the cell centers on the refined grid. The local topographic features are resolved in the model grid. The flow cells for rivers and canals and flood gates from the South Florida Water Management District are also displayed in (b).

observations for the better understanding of surge inundation (Soderqvist and Byrne 2007). This effort needs to be continued in the future when hurricanes approach the shore.

The improvement of simulations using finer-resolution grids while accounting for computation time has to be balanced for real-time forecasting. The simulation speed of the CEST model can be improved by parallelizing and distributing the CEST code to a cluster. However, in order to accommodate the uncertainty in track forecast, concurrent simulations of 2000–4000 tracks across affected basins using multiple CPUs with each CPU handling one or more cases is more practical for generating real-time P-Surge forecasts during the 48 h prior to landfall. The stability of the surge model is also important for real-time forecasting. One way to reduce the possibility of a model becoming unstable during an operational forecast run is to test the model against possible hurricanes affecting a basin. The CEST model has been tested for the nine Florida SLOSH basins using more than 100 000 tracks of synthetic hurricanes created by the NHC. Passing these tests ensures that the model will provide stable guidance in most cases, although there is no guarantee that the model will not have problems

during a real-time forecast. Therefore, it is safer to use at least two surge models (e.g., SLOSH and CEST) than to use one model to perform real-time forecasts. The other advantage to running multiple surge models is the ability to perform cross validation of simulations and to produce an ensemble forecast.

7. Summary and conclusions

The operational real-time forecasting of storm surge flooding requires that a numerical hydrodynamic model be capable of completing multiple surge simulations in minutes rather than in hours. Also, the numerical model must be highly stable and able to produce simulations in GIS format to facilitate the wide dissemination of computed storm surges. Therefore, in the process of transitioning a research model into an operational model, computational efficiency and numerical stability of the model, as well as the compatibility of the model products with operational guidance, must be considered in addition to accuracy. Such considerations have historically been lacking in traditional studies of hydrodynamic models. In this paper, a four-step procedure was developed for converting a hydrodynamic modeling system for

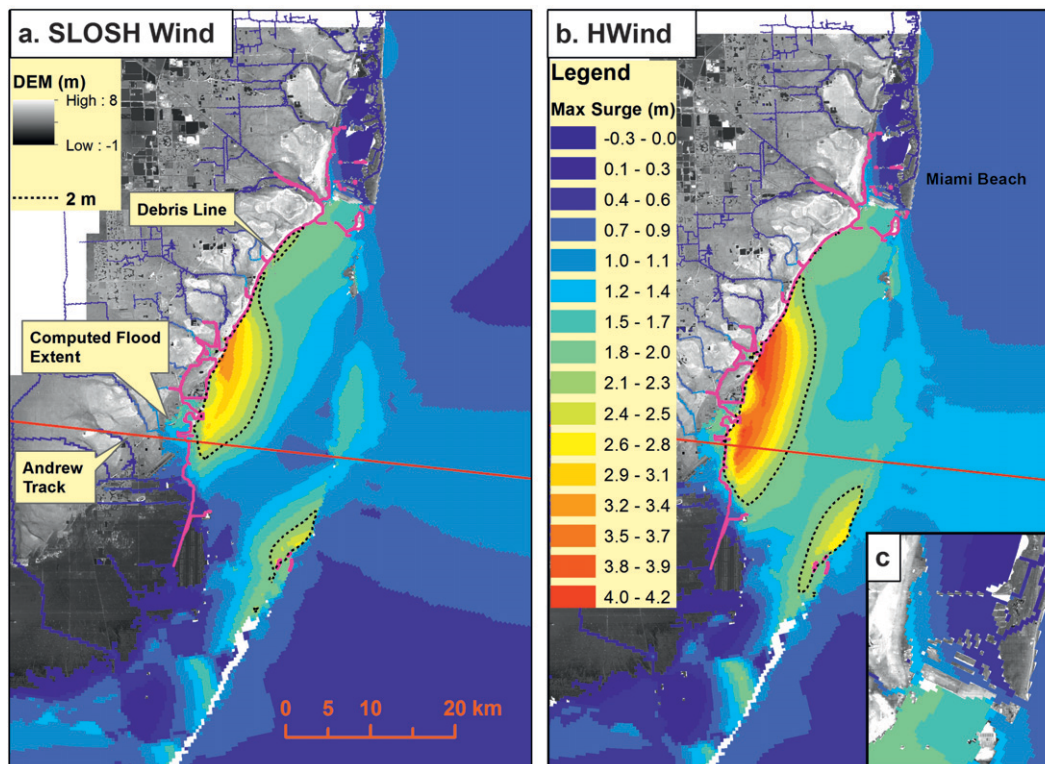


FIG. 11. The peak surge heights computed by CEST for the Miami basin using (a) the parametric SLOSH wind and (b) H*Wind. Inset (c) shows the zoomed-in view of the barrier island including Miami Beach shows that Dodge Island in the refined grid protected the bayside of Miami Beach from the surge inundation caused by Hurricane Andrew.

operational usage using CEST as an example. The four-step procedure includes 1) testing the feasibility of running CEST on existing SLOSH basins, 2) comparing the CEST and SLOSH simulations for individual historical storm events, 3) comparing the CEST and SLOSH simulations for multiple synthetic storms and recreating MEOWs and MOMs, and 4) examining the potential of CEST in improving surge forecasts by conducting simulations on refined SLOSH grids. This procedure has proven to be effective in exploring the process of transitioning CEST into an operational model and, therefore, provides a valuable reference to converting other research surge models into operational ones.

Surge simulations for more than 100 000 synthetic hurricanes affecting the coast indicate that CEST is numerically stable on the nine Florida SLOSH basins. Comparison of MEOW and MOM data indicates that CEST and SLOSH produce generally similar results in most cases. However, several distinct results were generated in a few cases because of the differences between SLOSH and CEST in handling the wetting–drying processes, bottom friction, and nonlinear items. CEST is capable of completing 72-h surge simulations on SLOSH

basins using a single 2.5-GHz Intel Xeon processor within 2 min in most cases, which is comparable to the computational speed of SLOSH. Therefore, the CEST model can be used to run real-time surge forecasts. The

TABLE 3. Computation times for 48-h simulations over various resolutions of grids. All simulations were performed using a PC workstation with four 2.5-GHz Intel Xeon processors and 12 GB of RAM, and each simulation was completed by using one processor.

No. of cells	Time step (s)	Running time (min)	Mean peak surge height (m)
126 × 191	60	0.7	0.430
126 × 191	30	1.4	0.432
126 × 191	20	1.9	0.434
252 × 382	60	4.3	0.432
252 × 382	30	6.9	0.433
252 × 382	20	9.3	0.434
378 × 573	40	16.6	0.430
378 × 573	30	19.3	0.431
378 × 573	20	24.8	0.431
378 × 573	10	42.7	0.433
504 × 764	30	43.0	0.431
504 × 764	20	54.1	0.432
504 × 764	10	79.6	0.432
1512 × 2292	5	2766.0	0.429

simulations conducted on the refined grids for the Miami basin demonstrate that CEST has the potential to produce more detailed real-time forecasts than those based on the current SLOSH grids.

The requirement for a new surge forecast system that is capable of conducting surge simulations on existing SLOSH basins and producing associated MEOW and MOM products is particularly useful for the surge forecast operation with the limited resources at the NHC. This capability would allow the NHC to potentially adopt an additional modeling system without incurring the cost associated with transitioning, building, and maintaining new model grids. This capability also allows the users of SLOSH surges to utilize the results from the new surge forecast system without significant additional training. Therefore, the four-step procedure is recommended for the conversion of the other research surge models into operational ones whenever it is possible. In addition, a fifth step, which involves the development of a set of tools to convert the outputs from multiple models into a standard GIS format and existing operational dissemination formats such as those used by the SLOSH display program, is worth exploring in the future to further facilitate the R2O transition of surge models.

Acknowledgments. Drs. Keqi Zhang, Yuepeng Li, and Huiqing Liu were supported by NOAA Grant NA09NWS4680018. We thank Drs. Edward Rapport and Chris Landsea at the NHC for reviewing the manuscript and providing valuable comments. We also thank three anonymous reviewers for valuable comments and suggestions. Discussion with Arthur Taylor and Dr. Harry Glahn at the MDL helped the corresponding author better understand the SLOSH model and the basin development process. Bobby Louangsaysongkham at the MDL provided ArcGIS shapefiles for SLOSH basins and an associated document. Michael Lowry at the NHC created Fig. 1. The findings and conclusions presented in this paper are entirely those of the authors and do not necessarily reflect the views of either the NHC or NOAA.

REFERENCES

- Blake, E. S., C. W. Landsea, and E. J. Gibney, 2011: The deadliest, costliest, and most intense United States tropical cyclones from 1851 to 2010 (and other frequently requested hurricane facts). NOAA Tech. Memo. NWS NHC-6, 49 pp.
- Blumberg, A. F., and L. Kantha, 1983: Open boundary condition for circulation models. *J. Hydraul. Eng.*, **112**, 237–255.
- , and G. L. Mellor, 1987: A description of three-dimensional coastal ocean circulation model. *Three-Dimensional Coastal Ocean Models*, N. S. Heaps, Ed., Coastal and Estuarine Sciences, Vol. 4, Amer. Geophys. Union, 1–16.
- Bunya, S., and Coauthors, 2010: A high-resolution coupled riverine flow, tide, wind, wind wave, and storm surge model for southern Louisiana and Mississippi. Part I: Model development and validation. *Mon. Wea. Rev.*, **138**, 345–377.
- Casulli, V., and R. T. Chen, 1992: Semi-implicit finite difference method for three-dimensional shallow water flow. *Int. J. Numer. Methods Fluids*, **15**, 629–648.
- , and R. A. Walters, 2000: An unstructured, three-dimensional model based on the shallow water equations. *Int. J. Numer. Methods Fluids*, **32**, 331–348.
- Chen, C., H. Liu, and R. C. Beardsley, 2003: An unstructured grid, finite-volume, three-dimensional, primitive equations ocean model: Application to coastal ocean and estuaries. *J. Atmos. Oceanic Technol.*, **20**, 159–186.
- Conver, A., J. Sepanik, B. Louangsaysongkham, and S. Miller, 2010: Sea, Lake, and Overland Surges from Hurricanes (SLOSH) basin development handbook v2.2. NOAA/NWS/Meteorological Development Laboratory, 76 pp.
- Forbes, C., and J. Rhome, 2011: An automated operational storm surge prediction system for the National Hurricane Center. *Proc. 12th Int. Conf. on Estuarine and Coastal Modeling*, St. Augustine, FL, American Society of Civil Engineers, 213–229.
- , J. G. Fleming, C. Mattocks, C. W. Fulcher, R. A. Luettich, H. J. Westerink, and S. Bunya, 2007: New developments in the ADCIRC community model. *Proc. 10th Int. Conf. on Estuarine and Coastal Modeling*, Newport, RI, American Society of Civil Engineers, 373–392.
- , R. A. Luettich, and C. Mattocks, 2009: Storm surge simulations of Hurricane Ike: Its impacts in Louisiana and Texas. *Proc. 11th Int. Conf. on Estuarine and Coastal Modeling*, Seattle, WA, American Society of Civil Engineers, 704–723.
- , —, —, and J. J. Westerink, 2010: A retrospective evaluation of the storm surge produced by Hurricane Gustav (2008): Forecast and hindcast results. *Wea. Forecasting*, **25**, 1577–1602.
- Fry, J., and Coauthors, 2011: Completion of the 2006 National Land Cover Database for the conterminous United States. *Photogramm. Eng. Remote Sens.*, **77**, 858–864.
- Glahn, B., A. Taylor, N. Kurkowski, and W. A. Shaffer, 2009: The role of the SLOSH model in National Weather Service storm surge forecasting. *Natl. Wea. Dig.*, **33** (1), 3–14.
- Haase, A., J. Wang, A. Taylor, and J. Feyen, 2011: Coupling of tides and storm surge for operational modeling on the Florida coast. *Proc. 12th Int. Conf. on Estuarine and Coastal Modeling*, St. Augustine, FL, American Society of Civil Engineers, 230–238.
- Hamrick, J., 1992: A three-dimensional environmental fluid dynamics computer code: Theoretical and computation aspects. Special Report in Applied Marine Science and Ocean Engineering 317, College of William and Mary, Virginia Institute of Marine Science, 63 pp.
- Huang, Y., R. H. Weisberg, and L. Zheng, 2010: Coupling of surge and waves for an Ivan-like hurricane impacting the Tampa Bay, Florida region. *J. Geophys. Res.*, **115**, C12009, doi:10.1029/2009JC006090.
- Irish, J. L., Y. K. Song, and K. A. Chang, 2011: Probabilistic hurricane surge forecasting using parameterized surge response functions. *Geophys. Res. Lett.*, **38**, L03606, doi:10.1029/2010GL046347.
- Jelesnianski, C. P., 1970: Bottom stress time-history in linearized equations of motion for storm surge. *Mon. Wea. Rev.*, **98**, 462–478.

- , J. Chen, and W. A. Shaffer, 1992: SLOSH: Sea, Lake and Overland Surges from Hurricanes. NWS Tech. Rep. 48, 71 pp.
- Kim, S. C., and J. Chen, 1999: Bottom stress of wind-driven currents over an inner shelf determined from depth-integrated storm surge model. *J. Coastal Res.*, **15**, 766–773.
- LeMehaute, B., 1976: *An Introduction to Hydrodynamics and Water Waves*. Springer-Verlag, 315 pp.
- Luetlich, R. A., J. J. Weserink, and N. W. Scheffner, 1992: ADCIRC: An advanced three-dimensional circulation model for shelves, coasts, and estuaries; Report I: Theory and methodology of ADCIRC-2DDI and ADCIRC-3DL. Dredging Research Program Tech. Rep. DRP-92-6, U.S. Army Corps of Engineers, 137 pp.
- Mattocks, C., and C. Forbes, 2008: A real-time, event-triggered storm surge forecasting system for the state of North Carolina. *Ocean Modell.*, **25**, 95–119.
- Murray, M. H., 1994: Storm-tide elevations produced by Hurricane Andrew along the southern Florida coasts, August 24, 1992. USGS Open-File Rep. 94–116, 27 pp.
- Murty, T. S., 1984: *Storm Surges: Meteorological Ocean Tides*. Vol. 212. Dept. of Fisheries and Oceans, 897 pp.
- Powell, M. D., S. H. Houston, L. R. Amat, and N. Morisseau-Leroy, 1998: The HRD real-time hurricane wind analysis program. *J. Wind Eng. Ind. Aerodyn.*, **77/78**, 53–64.
- , E. W. Uhlhorn, and J. D. Kepert, 2009: Estimating maximum surface winds from hurricane reconnaissance measurements. *Wea. Forecasting*, **24**, 868–883.
- Purray, R. J., and L. M. Leslie, 1988: A semi-implicit, semi-Lagrangian finite-difference scheme using high-order spatial differencing on a nonstaggered grid. *Mon. Wea. Rev.*, **116**, 2069–2080.
- Rego, J. L., and C. Li, 2008: On the importance of the forward speed of hurricanes in storm surge forecasting: A numerical study. *Geophys. Res. Lett.*, **36**, L07609, doi:10.1029/2008GL036953.
- Shaffer, W. A., C. P. Jelesnianski, and J. Chen, 1989: Hurricane storm surge forecasting. Preprints, *11th Conf. on Probability and Statistics in Atmospheric Sciences*, Monterey, CA, Amer. Meteor. Soc., J53–J58.
- Shen, J., K. Zhang, C. Xiao, and W. Gong, 2006: Improved prediction of storm surge inundation with a high-resolution unstructured grid model. *J. Coastal Res.*, **22**, 1309–1319.
- Sheng, Y. P., 1987: On modeling three-dimensional estuarine and marine hydrodynamics. *Three-Dimensional Models on Marine and Estuarine Dynamics*, J. C. J. Nihoul, and B. M. Jamart, Eds., Elsevier Oceanography Series, Vol. 45, Elsevier, 35–54.
- , V. Alymov, and V. A. Paramygin, 2010: Simulation of storm surge, wave, currents, and inundation in the Outer Banks and Chesapeake Bay during Hurricane Isabel in 2003: The importance of waves. *J. Geophys. Res.*, **115**, doi:10.1029/2009JC005402.
- Soderqvist, L., and M. Byrne, 2007: Monitoring the storm tide of Hurricane Wilma in southwestern Florida, October 2005. USGS Data Series 294, 16 pp.
- Taylor, A., and B. Glahn, 2008: Probabilistic guidance for hurricane storm surge. Preprints, *19th Conf. on Probability and Statistics*, New Orleans, LA, Amer. Meteor. Soc., 7.4. [Available online at <https://ams.confex.com/ams/pdfpapers/132793.pdf>.]
- , and C. Forbes, 2011: Implementation of a hybrid Laplacian filter in SLOSH to suppress numerical grid splitting. *Proc. 12th Int. Conf. on Estuarine and Coastal Modeling*, St. Augustine, FL, American Society of Civil Engineers, 348–358.
- Xie, L., L. J. Pietrafesa, and M. Peng, 2004: Incorporation of a mass-conserving inundation scheme into three-dimensional storm surge model. *J. Coastal Res.*, **20**, 1209–1223.
- Xu, H., K. Zhang, J. Shen, and Y. Li, 2010: Storm surge simulation along the U.S. East and Gulf Coasts using a multi-scale numerical model approach. *Ocean Dyn.*, **60**, 1597–1619.
- Zhang, K., C. Xiao, and J. Shen, 2008: Comparison of the CEST and SLOSH models for storm surge flooding. *J. Coastal Res.*, **24**, 489–499.
- , H. Liu, Y. Li, H. Xu, J. Shen, J. Rhome, and T. J. Smith III, 2012: The role of mangroves in attenuating storm surges. *Estuarine Coastal Shelf Sci.*, **102–103**, 11–23.
- Zhang, Y., and A. M. Baptista, 2008: SELFE: A semi-implicit Eulerian–Lagrangian finite-element model for cross-scale ocean circulation. *Ocean Modell.*, **21**, 71–96.
- , —, and E. P. Myers, 2004: A cross-scale model for 3D baroclinic circulation in estuary-plume-shelf systems: I. Formulation and skill assessment. *Cont. Shelf Res.*, **24**, 2187–2214.